7N05
97 198615

LIFT AND MOMENT INTERFERENCE OF WINGS AND BODIES

PART I - LIFT AND MOMENT INTERFERENCE AT ZERO

ANGLE OF BANK

Oct. 2 -3, 1951

By Jack N. Nielsen

Ames Aeronautical Laboratory

P-13

Moffett Field, Calif.

INTRODUCTION

Interference between the body and the lifting surfaces of a missile can have very large effects on its over-all aerodynamic characteristics, especially since the span of the missile is usually not large compared to its body diameter. Despite the very important influence that wing-body interference can have on lift and moment, no simple general method has hitherto been advanced for predicting these effects. The theories that have been advanced are of two types. Either they are complex mathematical solutions to boundary-value problems or they are approximate engineering methods.

The most useful theoretical results so far are those of Spreiter (reference 1) for slender plane and cruciform wing-body combinations. The results of Spreiter do not, however, apply directly to blunt missiles. Some mathematical solutions of various problems for rectangular wing-body combinations have been made by Ferrari, Morikawa, and Nielsen (references 2, 3, and 4), but these methods usually require much labor. A calculative technique of Nielsen and Matteson (reference 5) for determining interference pressure fields where interaction between the top and bottom surfaces of the wing does not affect the wing-body interference has been used by Moskowitz and Maslen (reference 6) to obtain the theoretical pressure distributions on a triangular and a rectangular wing-body combination. Comparison with experiment shows important effects of viscosity in the wing-body juncture. An approximate theory has been presented by Nielsen, Katzen, and Tang (reference 7) for obtaining the lift and moment characteristics of triangular wing-body combinations, and good agreement was obtained with experiment. Morikawa (reference 8) has presented approximate theories for triangular, rectangular, and trapezoidal wing-body combinations with no body behind the wing trailing edge.

To summarize the present situation, it can be said that the complicated mathematical theories are either too difficult or involve too much work to be useful in ordinary design and that the approximate methods are either too restrictive or involve unproved assumptions. There is thus a definite need for a simple engineering method of predicting lift

and moment interference effects for a wide range of practical configurations. It is the purpose of this paper to present a résumé of such a method together with an experimental verification of the method. The experimental data correlated with the theory include over-all lift and moment results for plane configurations and cruciform configurations at zero angle of bank.

SYMBOLS

a	body radius
c_r	chord at wing-body juncture
c_t	chord at wing tip
C_L	lift coefficient based on wing-alone area
C_N	normal-force coefficient based on wing-alone area
d	body diameter
K	ratio of lift of combination exclusive of nose to that of wing alone
K_B	ratio of lift of winged part of body to that of wing alone
K_W	ratio of lift of wing in combination to that of wing alone
L	lift force
M	free-stream Mach number
α	angle of attack
$\beta = \sqrt{M^2 - 1}$	
$\lambda = \dfrac{c_t}{c_r}$	
φ	angle of roll

Subscripts:

W	wing alone
B	body alone

W(B)   wing in presence of body

B(W)   body in presence of wing exclusive of nose

C   combination

C-N   combination exclusive of nose

LIFT AND MOMENT INTERFERENCE AT ZERO ANGLE OF BANK

Over-All Lift

First the over-all lift of wing-body combinations at zero angle of tank will be discussed, and then the over-all moment will be considered. In all cases the body and wing are rigidly attached. The manner used in this paper of specifying the lift of wing-body combinations is illustrated by figure 1. First, all lift forces are referred to the lift of the wing alone, which is taken as the exposed wing panels joined together. As a measure of the lift on the combination exclusive of the body nose, a factor K is introduced, which is the ratio of the lift developed on this part of the combination to the lift of the wing alone:

$$K = \frac{L_{C-N}}{L_W} \tag{1}$$

Similarly factors K_W and K_B are introduced to specify the lift of the wing in combination and the lift of the body in combination, exclusive of the nose:

$$K_W = \frac{L_{W(B)}}{L_W} \tag{2}$$

$$K_B = \frac{L_{B(W)}}{L_W} \tag{3}$$

$$K = K_B + K_W \tag{4}$$

It is clear that the determination of K_W and K_B is equivalent to determining the lift of the combination and its division between wing and body. The method used in determining K_W is now discussed.

Values of K_W can be estimated by slender-body theory or by strip theory using the upwash variation across the span of the wing caused by the body. A comparison of the values of K_W determined by the two theories plotted against radius-semispan ratio shows that strip theory is generally of the order of 10 percent higher than slender-body theory. However, strip theory is known to be too high since it assumes perfect reflection by the body. Therefore, K_W as given by slender-body theory has been used in the method of this paper. A curve giving the ratio K_W according to slender-body theory is presented in figure 2.

Hitherto the only theory for the determination of K_B was slender-body theory, but an alternate theory, of which use is made in this paper, is now described. For a wing mounted on a constant-diameter section, the lift is generated essentially by the wing. The lift so generated is carried over onto the body downstream of the Mach helix from the leading edge of the juncture. Behind the Mach helix from the trailing edge of the juncture not much lift is developed because of the influence of the wing trailing edge. Simplification of this nonplanar model is desirable for purposes of calculation. The assumption is thus made that the body is collapsed to a plane, and that the Mach helices become the Mach lines of figure 1. If it is further assumed that the wing panels act at their angle of attack and that the body area acts essentially at zero angle of attack, the value of K_B can be estimated by integrating the lift due to one wing panel over the area between the Mach lines, doubling the result, and dividing by the lift of the wing alone. This method is only applicable to cases where the wing tips have no lift contribution on the area considered, and when the body extends behind the trailing edge, that is, when there is an afterbody. The values of K_B determined by this method are in good accord with the slender-body values of K_B at the lower limiting aspect ratio where the wing tips just start to affect the wing-body interference, and they are more reliable at higher aspect ratios. The lower limiting aspect ratio is determined from the following equality

$$\beta A = \frac{4m\beta}{(1 + \lambda)(m\beta + 1)} \tag{5}$$

The values of K_B determined by the present theory were used for aspect ratios above the lower limiting aspect ratio, and the values of K_B given by slender-body theory were used below this aspect ratio. For highly tapered wings the lower limiting aspect ratio approaches zero, and in rare instances where the value of K_B given by the present theory exceeds that for slender-body theory near the lower limiting aspect ratio, the slender-body value is used. A simple design chart for the determination of K_B is included as figure 3.

The use of slender-body values of K_W and K_B together with the linear-theory values of the wing-alone lift-curve slope to determine the lift-curve slopes of wing-body combinations is termed "modified slender-body theory." Modified slender-body theory is in principle, although not in actual detail, that used in reference 7. The present theory differs from slender-body theory only in the use of new values of K_B for values of the aspect ratio greater than the lower limiting aspect ratio. The full details of the present method are included in reference 9.

To test the foregoing concepts, a correlation has been made between the complete-combination lift-curve slopes as measured and as predicted by the present method. The experimental results for the linear portion of the lift curve about zero angle of attack have been taken from many sources. The lift of the nose of the combinations has been predicted by slender-body theory. The correlation has been performed for about 100 wing-body, Mach wave configurations.

Figure 4 presents the correlation between estimated and experimental lift-curve slopes for 33 triangular wing-body combinations. The symbol β signifies the square root of the Mach number squared minus one. The line of perfect agreement is shown together with the limits of ±10 percent correlation. As can be seen, nearly all the configurations correlate within these limits. Figure 5 presents the correlation between the estimated and experimental lift-curve slopes for 20 rectangular wing-body configurations. Again nearly all the configurations fall within the ±10 percent correlation limits. Figure 6 shows the correlation curve for 41 trapezoidal wing-body configurations and again the correlation is about ±10 percent. The correlation curves include some configurations without afterbodies for which the present theory is not strictly applicable. On the average these configurations exhibit less experimental lift than estimated lift as would be expected. Detailed tables of the test conditions and aerodynamic coefficients of all the configurations correlated are included in reference 9.

Over-All Moment

To predict the over-all moment of a wing-body combination, it is necessary to predict the centers of pressure of the various components of the lift in addition to the components themselves. For the triangular wing-body combination the center-of-pressure positions have been calculated using the closed expression of Nielsen, Katzen, and Tang, reference 7, which is based entirely on slender-body theory and includes the effect of the body nose.

The correlation between the estimated and experimental center-of-pressure positions in body diameters behind the nose of the body is

presented in figure 7 for about 30 triangular wing-body combinations. Extremely good correlation is indicated, the scatter about the line of perfect agreement being only ±0.2 body diameter. The good agreement is believed to be the result of several compensating effects. First, slender-body theory does not take into account the tendency of the body to shift downstream the lift carried over onto it from the wing, thereby giving a position of the center of pressure that is too far forward. However, if a round afterbody behaves similarly to a flat one, there are negative lifting pressures on the rear of the afterbody which have the effect of moving the center of pressure forward. Good correlation between estimated and experimental center-of-pressure position for the triangular wings is thus fortuitous.

If slender-body theory is applied to rectangular wing-body combinations to determine the center of pressure of the exposed wing lift, it gives the erroneous result that the center of pressure is at the wing leading edge. Some theory other than slender-body theory is thus required for rectangular wing-body combinations. The lift components as given by the lift method of this paper were utilized. The center-of-pressure positions were calculated as follows: Slender-body theory was used to calculate the center-of-pressure position of the body nose. The center of pressure of the wing alone was used for the wing panels in combination. The center of pressure of the lift carried over on to the body by the wing was determined from the same calculative model already described for determining the lift.

Figure 8 shows the correlation between the estimated and experimental center-of-pressure positions for 18 rectangular wing-body combinations. This correlation curve illustrates the fact that the experimental center-of-pressure locations are on the average slightly forward of the estimated positions. This effect is believed to be due primarily to the afterbody which causes a forward shift in the actual center-of-pressure location, similar to that described for the triangular wing-body combinations.

At the present time no final results are available for the center-of-pressure positions for the trapezoidal wing-body combinations. A unified method for moment similar to that presented here for lift, to include triangular, rectangular, and trapezoidal combinations, is being attempted.

Left margin fragments:
ns.
le of
nt is

body
hereby
d.
re are
the

the

mbina-
, it
ing

nts as
of-
y was
. The
in
o the
ready

ri-
ombina-
imental
f the
to the
ssure

nter-
A
to
being

REFERENCES

1. Spreiter, John R.: Aerodynamic Forces on Slender Plane- and Cruciform-Wing and Body Combinations. NACA Rep. 962, 1950.

2. Ferrari, Carlo: Interference between Wing and Body at Supersonic Speeds - Theory and Numerical Application. Jour. Aero. Sci., vol. 15, no. 6, June 1948, pp. 317-336.

3. Morikawa, George: The Wing-Body Problem for Linearized Supersonic Flow. Progress Rep. No. 4-116, Jet Propulsion Lab., C.I.T., Dec. 19, 1949.

4. Nielsen, Jack N.: Supersonic Wing-Body Interference. Doctoral Dissertation, C.I.T., 1951.

5. Nielsen, Jack N., and Matteson, Frederick H.: Calculative Method for Estimating the Interference Pressure Field at Zero Lift on a Symmetrical Swept-Back Wing Mounted on a Circular Cylindrical Body. NACA RM A9E19, 1949.

6. Moskowitz, Barry, and Maslen, Stephen H.: Experimental Pressure Distributions over Two Wing-Body Combinations at Mach Number 1.9. NACA RM E50J09, 1951.

7. Nielsen, Jack N., Katzen, Elliott D., and Tang, Kenneth K.: Lift and Pitching-Moment Interference between a Pointed Cylindrical Body and Triangular Wings of Various Aspect Ratios at Mach Numbers of 1.50 and 2.02. NACA RM A50F06, 1950.

8. Morikawa, George: Supersonic Wing-Body Lift. Preprint No. 296, Inst. Aero. Sci., Inc., July 1950.

9. Nielsen, Jack N., and Kaattari, George E.: Method for Estimating Lift Interference of Wing-Body Combinations at Supersonic Speeds. (Prospective NACA paper)
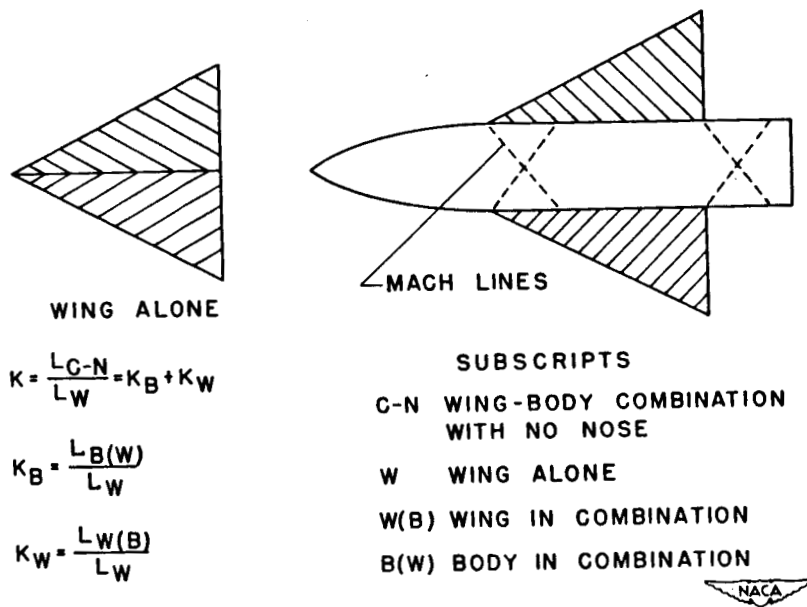
WING ALONE

$$K = \frac{L_{C-N}}{L_W} = K_B + K_W$$

$$K_B = \frac{L_{B(W)}}{L_W}$$

$$K_W = \frac{L_{W(B)}}{L_W}$$

MACH LINES

SUBSCRIPTS

C-N   WING-BODY COMBINATION WITH NO NOSE

W   WING ALONE

W(B) WING IN COMBINATION

B(W) BODY IN COMBINATION

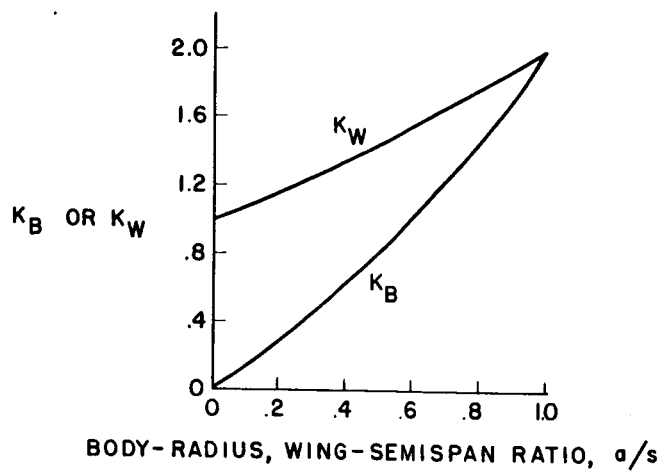NACA

Figure 1.- Symbols and definitions.

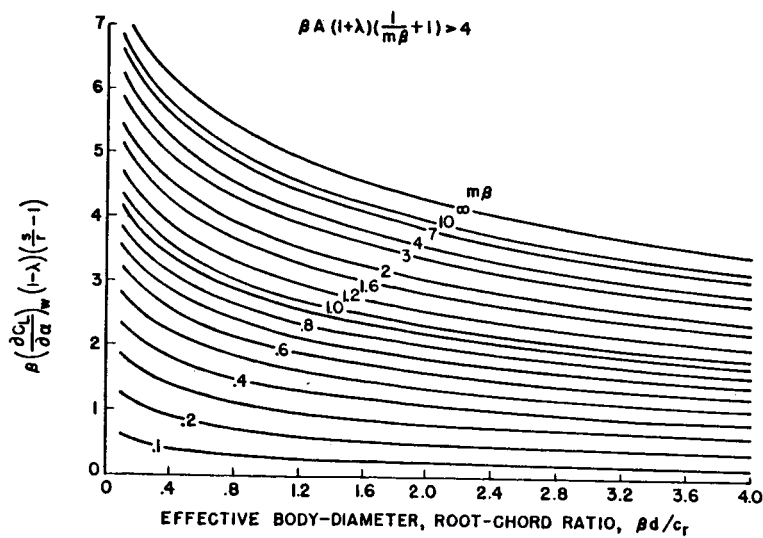Figure 2.- Chart for determining slender-body values for K_W and K_B.

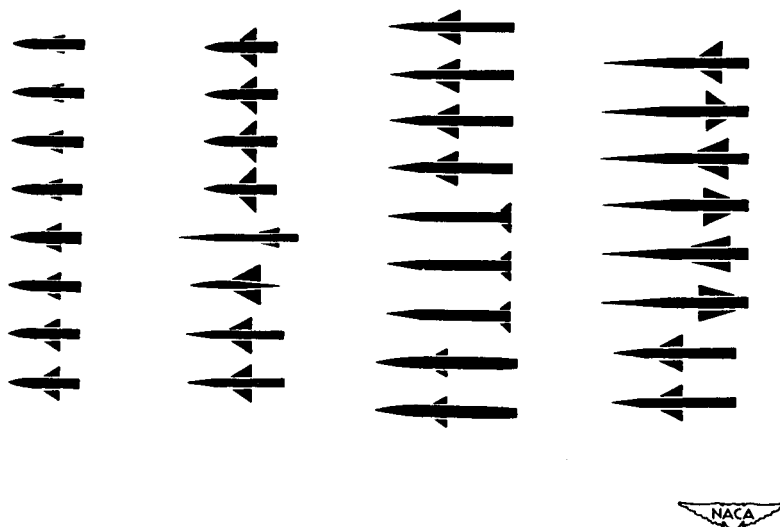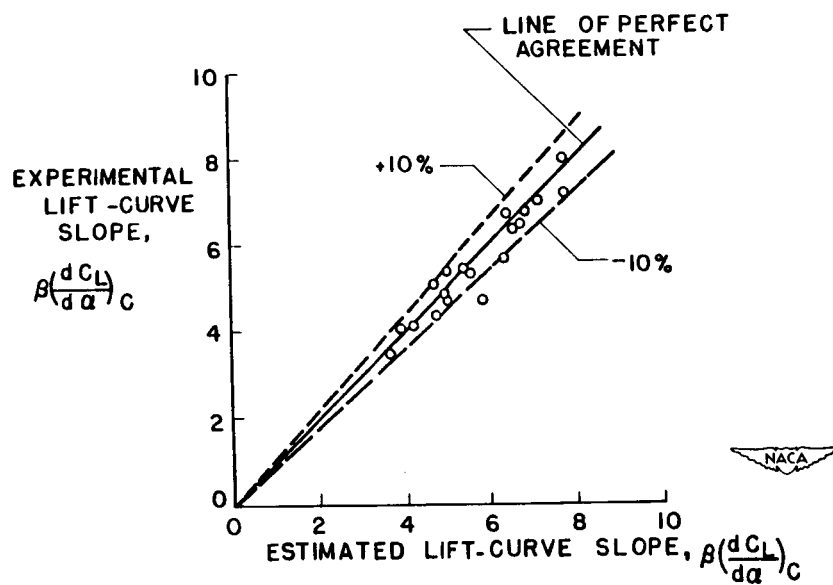Figure 3.- Chart for determination of K_B.
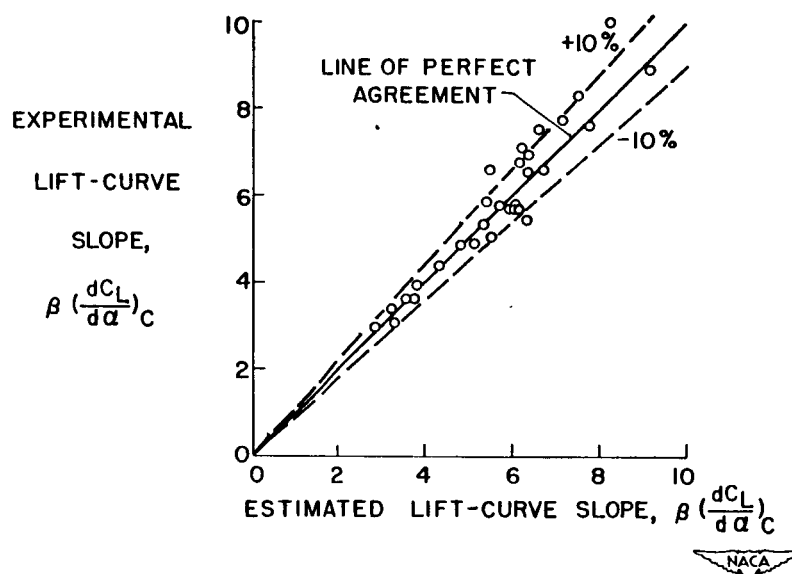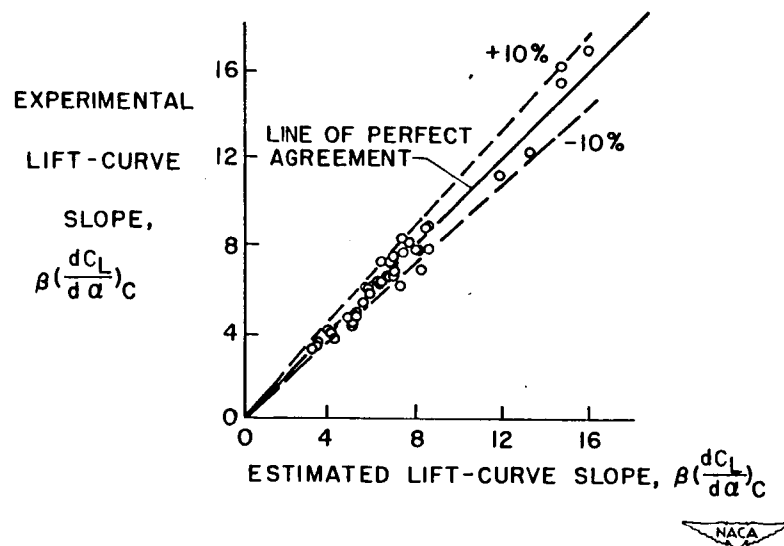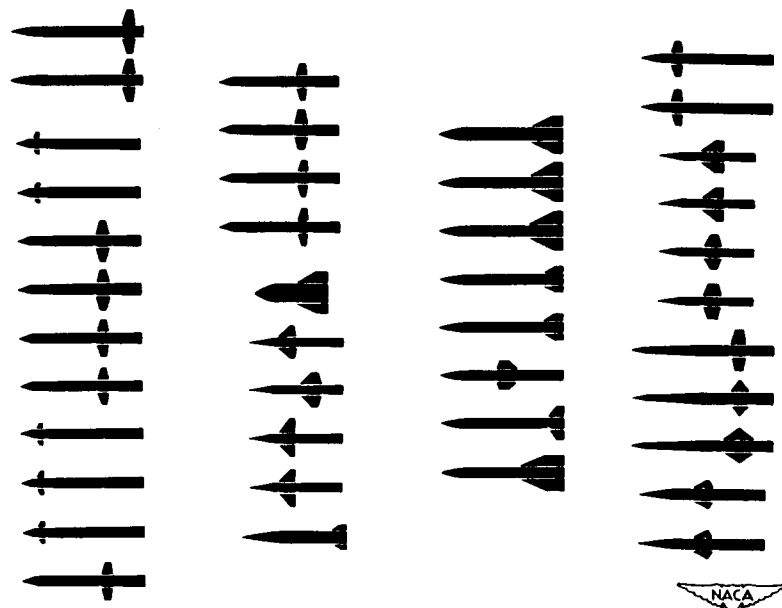
(a)   Correlation curve.

(b)   Triangular configurations correlated.

Figure 4.- Correlation between estimated and experimental lift-curve
slopes of triangular wing-body combinations.

(a)   Correlation curve.
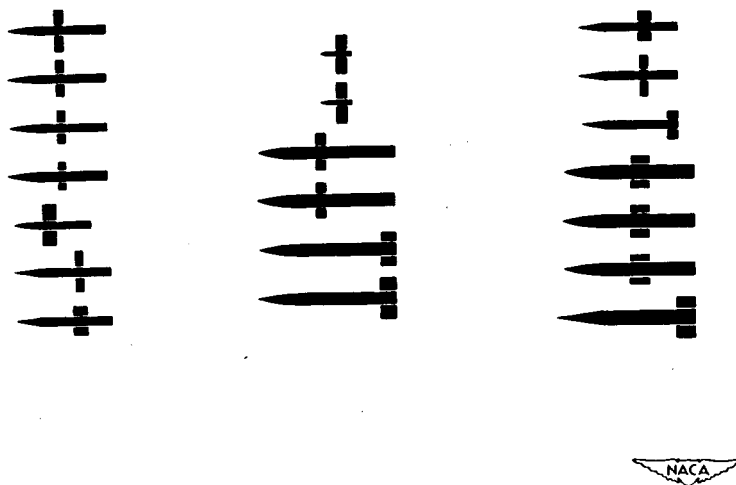
(b)   Rectangular configurations correlated.

Figure 5.- Correlation between estimated and experimental lift-curve
slopes of rectangular wing-body combinations.

(a) Correlation curve.

(b) Trapezoidal configurations correlated.

Figure 6.- Correlation between estimated and experimental lift-curve
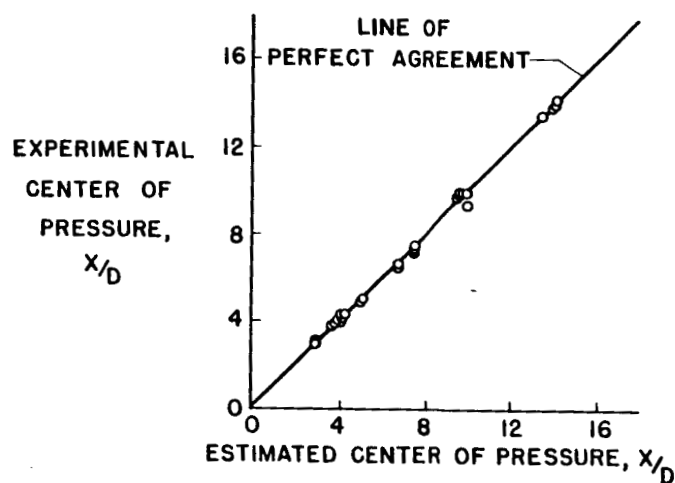slopes of trapezoidal wing-body combinations.

Figure 7.- Correlation between estimated and experimental centers of pressure for triangular wing-body combinations.
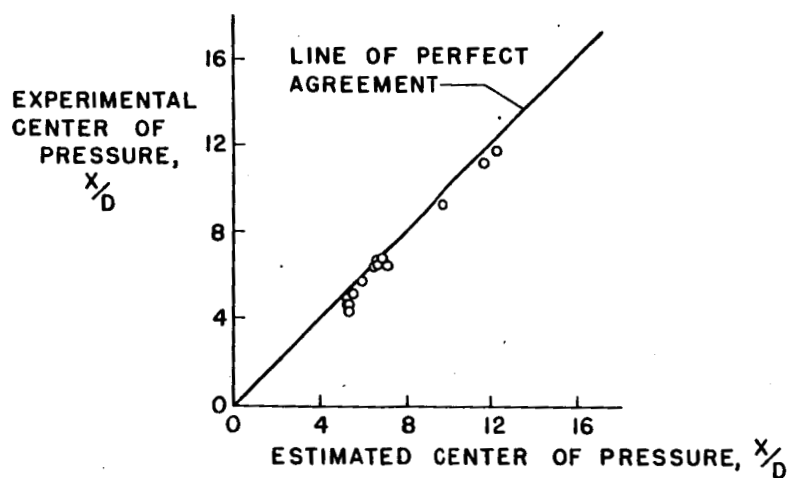

Figure 8.- Correlation between estimated and experimental centers of pressure for rectangular wing-body combinations.

e